RSC Advances

ROYAL SOCIETY OF CHEMISTRY

www.rsc.org/advances

RSC Advances

RSCPublishing

PAPER

Nitroxide radical polymer/carbon-nanotube-array electrodes with improved C-rate performance in organic radical batteries

Cite this: DOI: 10.1039/x0xx00000x

Received 00th January 2015,
Accepted 00th January 2015

DOI: 10.1039/x0xx00000x

www.rsc.org/

Chun-Hao Lin,[a] Jyh-Tsung Lee,*[ab] Dong-Rong Yang,[a] Hsiu-Wei Chen*[a] and Shao-Tzu Wu[a]

A poly(2,2,6,6-tetramethylpiperidin-1-oxy-4-yl methacrylate)/carbon-nanotube-array (PTMA/CNT-array) electrode was used as a cathode to improve the high-rate charge/discharge performance in organic radical batteries. Scanning electron microscopy observations showed that the PTMA/CNT-array electrode provides continuous conduction paths for electrons, and its electrochemical behaviours were investigated using cyclic voltammetry, charge/discharge tests, and AC impedance measurements. The results indicated that the PTMA/CNT-array electrode exhibits a lower electron-transfer resistance between CNTs and either the current collector or CNTs compared with conventional PTMA/suspended-CNT composite electrodes, enhancing the C-rate performance of batteries.

Keywords: Nitroxide polymer; Carbon nanotube array; Organic radical battery; Cathode; Redox polymer

Introduction

Nitroxide radical polymers are used as electrode-active materials in organic radical batteries, because of their excellent high-rate performance,[1] good cyclability,[2] high flexibility,[3] and thin-film properties.[4,5] In addition, they are able to structurally tailored , environmentally benign, and can be applied to various organic fabrication processes.[4] Poly(2,2,6,6-tetramethylpiperidin-1-oxyl-4-yl methacrylate)—PTMA—is a typical nitroxide radical polymer that is a suitable electrode-active material in organic radical batteries owing to its rapid charge-transfer process and high diffusion coefficient.[6,7] However, its poor electrical conductivity—a drawback of PTMA—limits the high-rate charge/discharge performance of batteries.[7,8]

To increase the electrical conductivity of PTMA electrodes, several carbon forms, including activated carbon,[9] Super P,[10] vapor-grown carbon fibers (VGCFs),[11] carbon black,[12] graphene,[13] and carbon nanotubes (CNTs),[14] are used as conductive additives. These are mixed with PTMA, a binder, and a solvent to form a viscous slurry coated onto a current collector. However, after the slurry is dried, the conductive carbon materials are coated with insulating polymers (PTMA and binder), inhibiting the conduction of electrons between conductive carbons and either the current collector or conductive carbons (Fig. 1a). Nishide and coworkers indicated that electron-transfer processes at the interface of current collector and conductive carbon influence the high-rate charge/discharge performance of batteries.[15,16] Therefore, a decrease in the electron-transfer resistance is required to enhance the electrochemical performance of the composite electrode. Among all conductive carbons, vertically aligned carbon nanotubes (VA-CNTs) with an intimate connection between the carbon nanotubes and current collector have shown to facilitate electrical conduction.[17, 18]

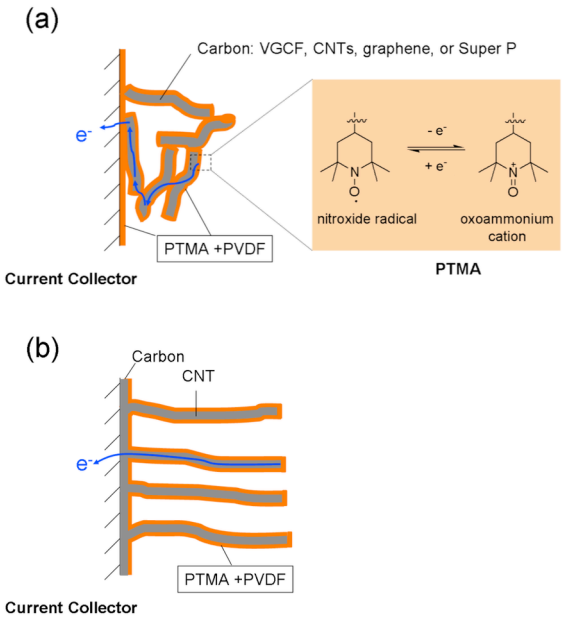

Fig. 1 Possible electron-conduction pathways for (a) PTMA/suspended-CNT composite electrode and (b) PTMA/CNT-array electrode.

In this paper, we use a VA-CNT-array on a current collector to provide continuous conduction paths for electrons, which prevents the insulator—PTMA or poly(vinylidene fluoride) (PVDF)—from blocking the conduction paths. Thus, the electron transfer resistance is effectively reduced and the batteries exhibit enhanced electrochemical performances (Fig. 1b). The surface morphologies of the electrodes were observed using scanning electron microscopy (SEM). The electrochemical properties of the electrodes were investigated using cyclic voltammetry (CV), C-rate tests, AC impedance measurements, and cycle-life performance measurements.

Experimental

Materials

Multiwalled CNTs (diameter 10–50 nm, length 5–20 μm; CNT Co., Ltd) and PVDF (Kuraha Chemical, KF 1100) were used without further purification. Ozone was generated on-site by an ozone generator (Fisher, Model 500, Germany) using 95% oxygen as the feed gas. PTMA was synthesized by free-radical polymerization (Mn = 44100 g mol^{-1}; polydispersity index = 1.84; radical concentration = 0.87). The theoretical capacity of PTMA is 111 mAh g^{-1}.[19]

Characterization

The surface morphologies of the electrodes were observed by field-emission SEM (JOEL JSM-6700F) operated at an accelerating voltage of 10 kV. Contact-angle measurements were performed on a Sindatek 100SB instrument. Electrochemical properties were obtained on a CHI model 6081 electrochemical instrument. Molecular weight was determined using gel permeation chromatography on a Shimadzu system with tetrahydrofuran (THF) using a Waters' Styragel® HR4 column at 45 °C. Radical concentrations were calculated from the peak area integrations of electron paramagnetic resonance spectra collected on a Bruker EMX-10 spectrometer.

Growth of VA-CNT-arrays

VA-CNT-arrays were grown on a 304 stainless-steel wafer via chemical vapor deposition (CVD) with ethene as the carbon source. The stainless steel wafer had a thickness of 0.1 mm and an area of 1 × 1 cm^2. Before CVD, the wafer was ultrasonicated in acetone for 15 min and washed with deionized water. Approximately 0.08 mL of 0.5 mM nickel acetate solution was dropped onto the wafer as a catalyst for CNT synthesis. The wafer was then dried in an oven at 160 °C for 20 min before placing it into the CVD reactor. The reactor was heated to 800 °C under flowing helium gas with a flow rate of 30 mL min^{-1}. CVD was then initiated with $C_2H_4/H_2/He$ = 1/1/8 by volume and a flow rate of 100 mL min^{-1} at 800 °C for 5 min. The reactor was cooled to room temperature under flowing helium before removing the sample for further treatment.

Ozone treatment of CNTs

The as-prepared VA-CNT-arrays and commercial multiwalled CNTs (0.3 g) were placed in a glass column connected to an ozone generator and ozone treated for 15 min at a flow rate of 3 g h^{-1}.

Fabrication of the PTMA/CNT-array and PTMA/suspended-CNT composite electrodes

For the PTMA/CNT-array electrode, an *N*-methyl-2-pyrrolidone (NMP) solution (1.0 g) of PTMA (3.0 mg) and PVDF (1.0 mg) was dropped onto the ozone-treated VA-CNT-array substrate. For the PTMA/suspended-CNT composite electrode, NMP slurry of PTMA (30 mg), PVDF (10 mg), and ozone-treated CNTs (60 mg) were ultrasonicated for 30 min and vigorously stirred for 30 min. The slurry was drop-casted onto a stainless-steel substrate with the VA-CNT-array grown on it. The PTMA/CNT-array and PTMA/suspended-CNT-composite samples were heated in a vacuum oven at 80 °C for 12 h to remove NMP. Note that the solid contents of both samples were similar (around 0.15 g cm^{-2}), and the amounts of PTMA, PVDF, and CNT in both electrodes were controlled to 30, 10, and 60 wt%, respectively. The prepared electrodes were not pressed to maintain pristine contact between the CNTs and current collectors.

Electrochemical measurements

Coin cells (CR2032) were assembled in an Ar-filled glove box. The PTMA/CNT-array or PTMA/suspended-CNT composite electrode was used as a cathode, and lithium metal was used as an anode. The separator was Celgard 2500 (polypropylene), and the electrolyte solution was 1.0 M $LiPF_6$ dissolved in ethylene carbonate (EC)/propylene carbonate (PC)/diethyl carbonate (DEC) (volume = 3/2/5) with 2% vinylene carbonate. CV experiments were conducted between 3.0 and 3.8 V at a scan rate of 1 mV s^{-1}. For AC impedance measurements, the perturbation amplitude was 5 mV, and the frequency range was 0.1–100 kHz. All electrochemical measurements were performed at 30 °C.

Results and discussion

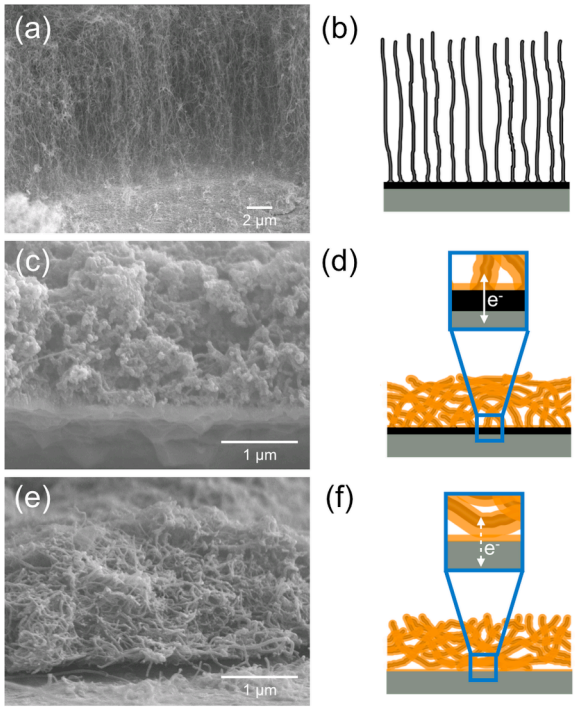

Fig. 2 SEM micrographs of (a) VA-CNT-array not been ozone treated, (c) PTMA/CNT-array electrode, and (e) PTMA/suspended-CNT composite electrode and their schematics (b), (d), and (f), respectively.

Figs. 2a, c, and e show SEM micrographs of the VA-CNT-array, PTMA/CNT-array, and PTMA/suspended-CNT-composite, respectively. These electrodes were prepared with similar compositions with 30% PTMA. The VA-CNT-array was prepared via CVD (Fig. 2a). CNTs were grown in parallel on the stainless-steel substrate, as illustrated in Fig. 2b. A VA-CNT-array with thickness of 20 μm was bound to the substrate. Fig. 2c obviously shows that the VA-CNT-array grew on a layer of carbon, which is typically seen in the CVD process.[20] Figs. 3a and b show the images of measuring the static water contact angle of an as-prepared VA-CNT-array substrate and the substrate after ozone treatment. The static water contact angle of the as-prepared VA-CNT-array was 150°, indicating that the array has a hydrophobic surface. It is difficult to homogenously coat the polar NMP slurry of PTMA and PVDF on CNTs with hydrophobic surfaces. To improve the wettability of the VA-CNT-array to PTMA and PVDF, the as-prepared VA-CNT-array was treated with ozone. After ozone treatment, the water contact angle of the VA-CNT-array was 30°, indicating that the ozone-treated VA-CNT-array became polar. PTMA and PVDF were then homogenously coated onto the VA-CNT-array to yield a PTMA/CNT-array electrode. Although the structure of the VA-CNT-array collapsed after coating with PTMA, the bases of the CNTs remained tightly bound to the substrate (Fig. 2c). As illustrated in Fig. 2d, after coating with PTMA, the bonds between the CNTs and the substrate provided continuous conduction paths for electrons. However, Fig. 2e shows that the PTMA/suspended-CNT composite electrode did not tightly contact the current collector. The electrical conduction paths were blocked by PTMA and PVDF that are poor electrical conductors between CNTs and the current collector (Fig. 2f). Therefore, the electrical resistance of the PTMA/suspended-CNT composite electrode was greater than that of the PTMA/CNT-array electrode. We believe that the PTMA/CNT-array electrodes exhibit lower electron-transfer resistance between the current collector and CNTs, leading to good electrochemical performance.

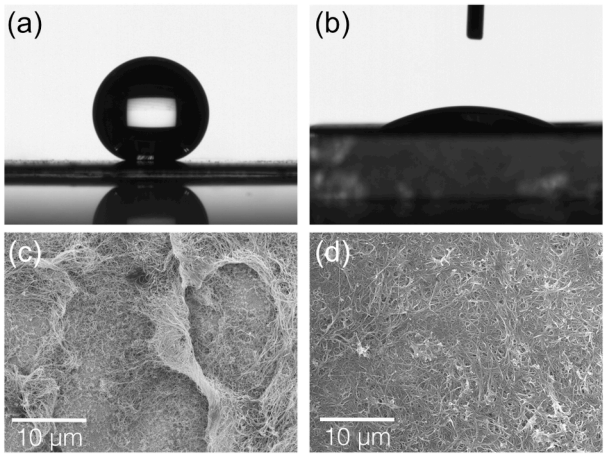

Fig. 3 Water static contact angle images of a VA-CNT-array substrate: (a) as-prepared and (b) after ozone treatment. (c) and (d) Top-view SEM images showing the different morphologies of polymeric materials drop casted on the as-prepared and ozone-treated VA-CNT-arrays, respectively.

Fig. 4a shows the cyclic voltammograms for the PTMA/CNT-array and PTMA/suspended-CNT composite electrodes, which reveal a redox couple at approximately 3.6 V vs. Li/Li+; this is a typical redox potential of nitroxide radicals and oxoammonium cations.[10] The voltammogram of the PTMA/CNT-array electrode exhibits a smaller peak-separation potential, indicating a rapid charge transfer in the electrochemical processes. This may be attributed to the continuous conduction path for electrons. Figs. 4b and c show the charge/discharge curves of the PTMA/CNT-array and PTMA/suspended-CNT composite electrodes, respectively, at different C-rates. A flat plateau at 3.5–3.7 V is observed in each charge/discharge curve, which is in good agreement with the typical PTMA charge/discharge curve.[10] At the discharge rate of 1 C, the discharge capacity of both electrodes was approximately 80–90 mAh g^{-1}. At the discharge rate of 100 C, the discharge capacity of the PTMA/CNT-array electrode was 63 mAh g^{-1} and that of the PTMA/suspended-CNT composite electrode decreased to 49 mAh g^{-1}. For high-C-rate discharge tests, the discharge capacity of the PTMA/CNT-array electrode was greater than that of the PTMA/suspended-CNT composite electrode. Since the carbon additives in both electrodes are ozone-treated CNTs, they should have similar effective areas. The difference between the discharge capacities under high C-rate may be due to the lower resistance of the continuous conduction path for electrons. In addition, a comparison of the voltages of the charge/discharge curves reveals that the PTMA/CNT-array electrode exhibited a smaller IR drop than the PTMA/suspended-CNT composite electrode at a high discharge rate. These results imply that the PTMA/CNT-array electrodes provide continuous conduction paths for electrons, reducing the electrical resistance; this coincides with the observed SEM and CV results. For cycle-life performance, Fig. 4d reveals that the discharge capacity of both electrodes after 100 cycles was approximately 80 mAh g^{-1}, indicating good cycle-life performance.

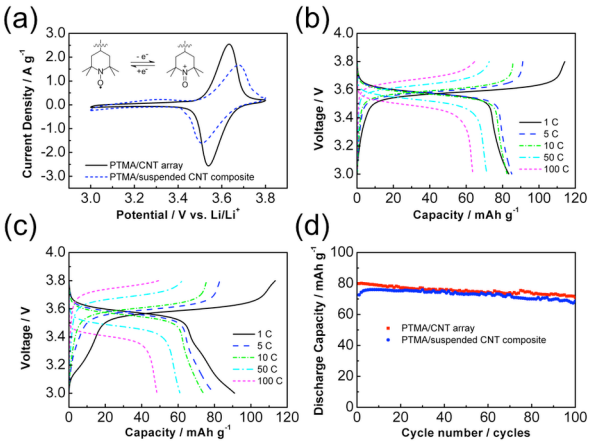

Fig. 4 (a) Cyclic voltammograms for the PTMA/CNT-array and PTMA/suspended-CNT composite electrodes; charge/discharge curves of (b) PTMA/CNT-array and (c) PTMA/suspended-CNT composite electrodes at C-rates 1, 5, 10, 50, and 100 C; (d) cycle-life performance of PTMA/CNT-array and PTMA/suspended-CNT composite electrodes.

To further investigate the differences between electrode impedances, AC impedance measurements were performed. Fig. 5a shows Nyquist plots for the PTMA/CNT-array and PTMA/suspended-CNT composite electrodes in assembled cells. The results show that the diameter of a quasi-semicircle

along the real axis may include the resistances of charge transfer and solid-electrolyte interface (SEI) films of electrodes. In the anode, the resistances of the SEI films on the lithium electrodes of both cells may be similar. The PTMA/CNT-array electrode has a smaller diameter than the PTMA/suspended-CNT electrode. Therefore, the charge-transfer resistance of the PTMA/suspended-CNT electrode is greater. To investigate the impedance in the Nyquist plots in detail, we used equivalent circuits, as shown in Fig. 5b. The overall impedance includes the electrolyte resistance (R_s), SEI resistance (R_{SEI}), charge-transfer resistance (R_{ct}), and Warburg impedance (W). Constant-phase elements (CPE_{SEI} and CPE) were used to account for an imperfect double-layer capacitance. The fitting results were obtained by ZView version 3.2c. The simulated results agreed well with the experimental results. The results show that the R_s value of both electrodes was 3.2 Ω cm^2, because both used the same electrolyte; the R_{SEI} value of both electrodes was approximately 80–100 Ω cm^2. As stated above, the value of R_{SEI} can be primarily attributed to the SEI resistance of the lithium electrode. Therefore, these resistances for both electrodes are very similar. However, the R_{ct} values of the PTMA/CNT-array and PTMA/suspended-CNT composite electrodes were 100 Ω cm^2 and 500 Ω cm^2, respectively, which are significantly different. The charge-transfer resistance for the PTMA/CNT-array electrode was lower than that of the PTMA/suspended-CNT composite electrode. We believe that the CNT-array is in direct contact with the stainless-steel current collector. This direct contact facilitates the reduction of the electron-transfer resistance between CNTs and either the current collector or CNTs, resulting in the reduction of the R_{ct} value of the PTMA/CNT-array electrode. This decrease also confirms the electrochemical behaviors observed in the CV and charge/discharge test results.

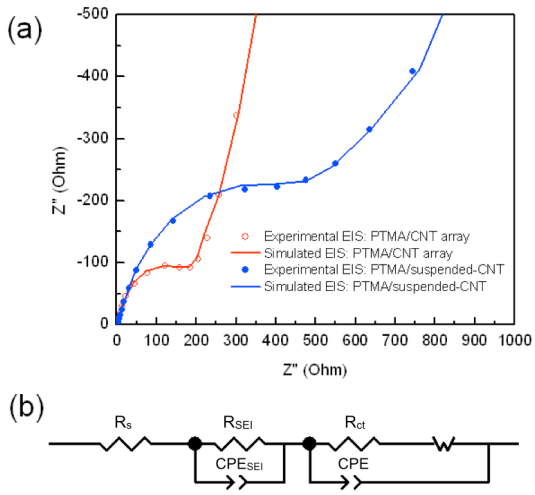

Fig. 5 (a) Nyquist plots and (b) equivalent circuit model of lithium coin cells with PTMA/CNT-array and PTMA/suspended-CNT composite electrodes.

Conclusions

We demonstrated a novel PTMA/CNT-array electrode with improved electrochemical performance in organic radical batteries. Compared with conventional PTMA/suspended-CNT composite electrodes, the new electrode provides continuous conduction paths for electrons, resulting in decreased electrode resistance. Moreover, the electrochemical measurement results show that the discharge capacity of the PTMA/CNT-array electrode is 63 mAh g^{-1} at 100 C, which is greater than that of the conventional PTMA/conductive-additive composite electrode. The PTMA/CNT-array electrode cells exhibit a promising cycle-life performance with 98.0% capacity retention after 100 C. The results of AC impedance measurements confirm the low charge-transfer resistance of the PTMA/CNT-array electrode, which may be due to the low electron-transfer resistance between CNTs and either the current collector or CNTs.

Acknowledgements

The authors are grateful for financial support from the Ministry of Science and Technology, Taiwan.

Notes and references

[a] Department of Chemistry, National Sun Yat-Sen University, Kaohsiung, Taiwan. 70, Lienhai Rd,. Gushan Dist., Kaohsiung City 80424, Taiwan.
[b] Department of Medicinal and Applied Chemistry, Kaohsiung Medical University, Kaohsiung 80708, Taiwan. 100, Shih-Chuan first Rd., Kaohsiung City 80708, Taiwan
Fax: +886-75253951 E-mail: jtlee@faculty.nsysu.edu.tw (J.-T. Lee); hwchen@faculty.nsysu.edu.tw (H.-W. Chen)

1. K. Nakahara, J. Iriyama, S. Iwasa, M. Suguro, M. Satoh and E. J. Cairns, *J. Power Sources*, 2007, **165**, 870-873.
2. J.-K. Kim, J.-H. Ahn, G. Cheruvally, G. Chauhan, J.-W. Choi, D.-S. Kim, H.-J. Ahn, S. Lee and C. Song, *Met. Mater. Int.*, 2009, **15**, 77-82.
3. T. Suga, H. Ohshiro, S. Sugita, K. Oyaizu and H. Nishide, *Adv. Mater.*, 2009, **21**, 1627-1630.
4. T. Suga, H. Konishi and H. Nishide, *Chem. Commun.*, 2007, 1730-1732.
5. Y.-H. Wang, M.-K. Hung, C.-H. Lin, H.-C. Lin and J.-T. Lee, *Chem. Commun.*, 2011, **47**, 1249-1251.
6. K. Oyaizu and H. Nishide, *Adv. Mater.*, 2009, **21**, 2339-2344.
7. H. Nishide and T. Suga, *Electrochem. Soc. Interface*, 2005, **14**, 32-35.
8. L. Rostro, A. G. Baradwaj and B. W. Boudouris, *ACS Appl. Mater. Interfaces*, 2013, **5**, 9896-9901.
9. E. Lebègue, T. Brousse, J. Gaubicher, R. Retoux and C. Cougnon, *J. Mater. Chem. A*, 2014, **2**, 8599-8602.
10. J.-K. Kim, G. Cheruvally, J.-H. Ahn, Y.-G. Seo, D. S. Choi, S.-H. Lee and C. E. Song, *J. Ind. Eng. Chem.*, 2008, **14**, 371-376.
11. H. Nishide, S. Iwasa, Y.-J. Pu, T. Suga, K. Nakahara and M. Satoh, *Electrochim. Acta*, 2004, **50**, 827-831.
12. K. Nakahara, J. Iriyama, S. Iwasa, M. Suguro, M. Satoh and E. J. Cairns, *J. Power Sources*, 2007, **165**, 398-402.
13. W. Guo, Y.-X. Yin, S. Xin, Y.-G. Guo and L.-J. Wan, *Energy Environ. Sci.*, 2012, **5**, 5221-5225.
14. W. Choi, S. Ohtani, K. Oyaizu, H. Nishide and K. E. Geckeler, *Adv. Mater.*, 2011, **23**, 4440-4443.
15. S. Yoshihara, H. Isozumi, M. Kasai, H. Yonehara, Y. Ando, K. Oyaizu and H. Nishide, *J. Phys. Chem. B*, 2010, **114**, 8335-8340.
16. S. Yoshihara, H. Katsuta, H. Isozumi, M. Kasai, K. Oyaizu and H. Nishide, *J. Power Sources*, 2011, **196**, 7806-7811.
17. H. Zhang, G. Cao, Z. Wang, Y. Yang, Z. Shi and Z. Gu, *Electrochim. Acta*, 2010, **55**, 2873-2877.

18. H. Zhang, G. Cao, Z. Wang, Y. Yang, Z. Shi and Z. Gu, *Electrochem. Solid-State Lett.*, 2008, **11**, A223-A225.
19. C.-H. Lin, C.-M. Chau and J.-T. Lee, *Polym. Chem.*, 2012, **3**, 1467.
20. G. D. Nessim, *Nanoscale*, 2010, **2**, 1306-1323.